STREAMFLOW PREDICTION BASED ON DATA-SCARCE RIVER-AQUIFER DYNAMICS ESTIMATED BY A SIMPLIFIED MODELLING FRAMEWORK IN A DRYLAND CATCHMENT

Arthur J. de A. Toné[1]; Alexandre C. Costa[2]; Mário U. G. Barros[3]; Iran E. Lima Neto[4]

Abstract: Water security relies on accurately representing hydrological processes in river-aquifer dynamics, including aquifer recharge driven by rainfall, hyporheic flow, and lateral tributary inflows. River–aquifer studies often overlook these processes, however. Using a parsimonious numerical model, we accurately calculated these processes in a data-scarce region, at scales relevant to water management. This model was developed based on a conceptual model of river-aquifer dynamics in dryland regions. The numerical model's performance measures (Kling-Gupta efficiency, Nash–Sutcliffe efficiency, and percent bias) showed that it effectively estimated river and groundwater flow using a simple modeling approach, requiring only minimal calibration (three parameters). Notably, the data required for the model are often available in regions with scarce data availability. Hyporheic flow is crucial for the water balance in dryland rivers. In contrast, subcatchment runoff demonstrated minimal influence compared to inflow and groundwater fluxes, suggesting a greater dependence on river volume and stage than on intraseasonal rainfall. This study provides valuable tools for similar areas that require viable management solutions to be developed.

Keywords: River-aquifer interaction. Flow routing. River loss.

Resumo: A segurança hídrica depende da representação precisa dos processos hidrológicos nas dinâmicas rio-aquífero, incluindo a recarga do aquífero induzida pela precipitação, o fluxo hiporreico e as afluências laterais de tributários. Contudo, esses processos são frequentemente negligenciados em estudos sobre a interação rio-aquífero. Neste trabalho, utilizou-se um modelo numérico parcimonioso para calcular com precisão tais processos em uma região com escassez de dados, em escalas relevantes para a gestão dos recursos hídricos. O modelo foi desenvolvido com base em um modelo perceptual das dinâmicas rio-aquífero em regiões semiáridas. Os indicadores de desempenho do modelo numérico — eficiência de Kling-Gupta, eficiência de Nash–Sutcliffe e viés percentual — demonstraram que ele estimou de forma eficaz os fluxos de água superficial e subterrânea por meio de uma abordagem de modelagem simples, exigindo calibração mínima (três parâmetros). Destaca-se que os dados necessários para a aplicação do modelo são comumente disponíveis mesmo em contextos de escassez de dados. O fluxo hiporreico revelou-se essencial para o balanço hídrico em rios de regiões áridas. Em contraste, a contribuição do escoamento de sub-bacias mostrou-se mínima quando comparada às afluências e aos fluxos subterrâneos, sugerindo uma maior dependência do volume e da lâmina do rio do que das chuvas intraestacionais. Este estudo oferece ferramentas valiosas para áreas similares que necessitam de soluções viáveis de gestão.

INTRODUCTION

[1] Federal Institute of Education, Science and Technology - IFCE: Email: arthur.jordan@ifce.edu.br
[2] University of International Integration of the Afro-Brazilian Lusophony - UNILAB: Email: cunhacos@unilab.edu.br
[3] Water Resources Management Company of Ceará - COGERH. Email: mario.barros@cogerh.com.br
[4] Federal University of Ceará – UFC: Email: iran@deha.ufc.br

Various numerical models have been developed over the last few decades to simulate river-aquifer dynamics, as their behavior affects agricultural, industrial, and domestic purposes (Chen *et al.* (2020)). Although numerical models constitute reliable approaches to understanding river-aquifer water fluxes, current state-of-the-art challenges still require reliable answers. Two of them are particularly important for dryland regions: (a) high dependency on and frequency of field measurements, and (b) a parsimonious approach to favor calibration on a daily time step, which is critical for efficient management policies and river operations (Kim *et al.* (2022)). Moreover, water security depends on an adequate representation of the hydrological processes involved in river-aquifer dynamics, such as the behavior of groundwater levels in response to rainfall, hyporheic flow to the river, and lateral tributary inflow (sub-catchment runoff to the river). These processes represent a research gap, as they are often neglected in river-aquifer studies (Hussain *et al.* (2022)).

In this study, we propose a numerical model to estimate streamflow for data-scarce catchments. This model is based on a conceptual model proposed for dryland regions, and it can mimic river-aquifer dynamics by addressing the above-mentioned challenges, that is, modelling data-scarce environments and representing the often-overlooked processes involved in groundwater flow response to rainfall. Additionally, this study contributes to improving the understanding of the processes involved in river-aquifer dynamics, as it offers a more accurate water balance at the river-aquifer scale, which is crucial for adequate daily water management in dryland-based communities.

The study's research objectives are

(1) To formulate a conceptual model of the dominant processes in river-aquifer dynamics in data-scarce regions.
(2) To develop a parsimonious numerical model capable of simulating the processes involved in river-aquifer dynamics in a dryland catchment at temporal and spatial scales that are important for water management.
(3) To provide insight into the overlooked processes related to river losses and gains in large dryland rivers, such as lateral tributary inflow and hyporheic flow.

DATA AND METHODS

Study area

The study site is a mixed flow system, losing/gaining reach of the Middle Jaguaribe River in Ceará, NE-Brazil. The Köppen classification system characterizes the region as having a hot, semi-arid climate with a distinct contrast between the dry and rainy seasons. The study river drains an area of 2,898 km² and extends for a total length of 70.91 km, divided into three river reaches between gauging stations (N1, N2, N3, and N4): N1 to N2 (34.72 km), N2 to N3 (15.23 km), and N3 to N4 (20.96 km). The river slopes range from 0.03 m/km between N2 and N3 to 0.94 m/km between N3 and N4, with the reach between N1 and N2 exhibiting an intermediate value of 0.59 m/km (CPRM (2014, 2015)). The studied river primarily relies on contributions at its entrance (N1 gauge) from the Salgado River and water release from the Orós Reservoir, which has a total drainage area of 38,000 km².

Unconfined aquifers predominantly underlie the simulated river reaches, which are part of an alluvial system with a maximum depth of 30 m and a mean grain size of 0.90 mm. These aquifers connect hydraulically to the underlying crystalline rock formations, which do not support significant regional groundwater flow (Wiegand (2009)).

Datasets

The geometric shape of the river cross section is triangular for practical purposes. Once the river stage head was measured (see below), geometric parameters (area, perimeter, top width, and hydraulic radius) were derived from this shape. The top width of cross section was assumed to be constant when no flow was beyond the main channel. The Copernicus GLO-30 digital elevation model was used in the QGIS raster analysis tool to determine the channel length, slope, and sub-catchment area. The curve number of the sub-catchments was derived from raster data type of land use in Brazil provided by the National Water and Sanitation Agency of Brazil (ANA (2018)), incorporating a type 2 precondition concerning soil moisture. The hydraulic conductivity of the riverbed was estimated using Hazen's method and the riverbed grain size in the study area provided by Wiegand (2009). The hydraulic conductivity of alluvium and aquifer width were collected from hydrogeological surveys provided by the Brazilian Geological Service (CPRM).

The inflow and river stages were measured daily using an Acoustic Doppler Current Profiler (SonTek RiverSurveyor M9 ADCP) throughout the first semester of 2022 (from 04 January 2022 to 21 June 2022) at N1, N2, N3, and N4 to generate their rating curves. Subsequently, the water level (m) was measured daily at N1, N2, and N3 during the first semester of 2023 (from 01 January 2023 to 09 May 2023), and the rating curves were used to compute the inflow (m^3/s). Daily measurements at the N4 gauge in 2023 were unavailable owing to technical difficulties. We also encountered similar technical issues at the N2 gauge starting 10 May 2023. The daily volume, however, was measured during the first half of 2022 and 2023 within a 24-hour interval, starting at 07:00 on the day before the measurement. Daily rainfall data for the study site were accessible through the Ceará Foundation of Meteorology and Water Resources (FUNCEME) (see http://www.funceme.br/app-calendario/). We computed average rainfall using the Thiessen Polygons method with FUNCEME's Hydrological Calculation software, "SIGA" (see http://www.siga.funceme.br). Daily evaporation data were obtained from the National Institute of Meteorology (INMET) at the Jaguaribe station (see https://bdmep.inmet.gov.br/), near the N3 gauge.

River routing

We developed an original river routing model based on a nonlinear variation of the Muskingum-Cunge method proposed by Lu *et al.* (2021). For each of the three reaches, streamflow along the Δx river length at each Δt time step—accounting for a one-day lag between river gauges—is calculated as follows:

$$Q_{t+\Delta t} = \frac{1}{1-X}\left(\frac{S_t}{K}\right)^{\frac{1}{\gamma m}} - \frac{X \cdot I_t + \pi + \mu + \Omega + \partial}{1-X} \quad (1)$$

Where $Q_{t+\Delta t}$ represents the outflow (m^3/s), S_t denotes the storage volume (m^3), K is the storage constant (s), X is the weighting factor, γ and m are the calibrated exponents that relate storage and weighted flow, and I_t is the inflow (m^3/s). Gauged flow and volume data were used for all S_t and I_t values for each reach. Additionally, π represents the direct flux within the river (m^3/s), μ denotes the sub-catchment runoff (m^3/s), and Ω represents the river-aquifer interaction (m^3/s). δ is the volume of water used to meet the demand within each river reach, including groundwater extraction from operational wells and direct pumping from the river (m^3/s), which were considered insignificant at the study site. We propose the following rules for the γ value.

$$\begin{cases} \text{if } h_{river} \leq h_{r,m}, \text{ then } \gamma = \gamma^{+} \\ \text{if } h_{river} > h_{r,m}, \text{ then } \gamma = \gamma^{-} \end{cases} \quad (2)$$

Where h_{river} represents the river head (m), $h_{r,m}$ represents the mean river head at the river's entrance boundary (m), and γ+ and γ- represent the γ values that increase or decrease the relationship between storage and weighted flow. In this context, the calibration process requires only three parameters for computing the numerical model: m, γ+, and γ−. We calculated K and X using the equations of the original Muskingum-Cunge method, as presented by Fread (1993).

We compute the π component using the equation of Kim *et al.* (2022) modified:

$$\pi = a_{riv} \cdot (e - p) \quad (3)$$

$$a_{riv} = B \cdot \Delta x \quad (4)$$

Where a_{riv} represents the river area (m^2), and e (mm) and p (mm) denote evaporation and rainfall, respectively. We calculate the μ component using the SCS-CN method, and its maximum value for each river reach was defined as the average daily inflow measured during the first halves of 2022 and 2023. The ANA (2018) raster data type (see Datasets) determines CNj. Subsequently, if required, CNj is adjusted based on the actual moisture precondition (type 1 or 3) in response to the previous daily rainfall (p).

Groundwater flow

The aquifer stage head must first be estimated to calculate the river-aquifer interaction term (Ω). The scarcity of field measurements of groundwater in the semi-arid region of Brazil (Costa *et al.* (2023); Kim *et al.* (2022)) led us to utilize the analytical solution for aquifer heads proposed by Chesnaux *et al.* (2005) for unconfined aquifers (Equation 5) owing to its versatility and accuracy. This solution is based on Darcy's law and the Dupuit theory. It considers an impermeable boundary surrounding the aquifer, with a fixed-head boundary on the side adjacent to the river. As mentioned above, the river cross-section was assumed triangular.

$$h_{aq} = \sqrt{\frac{WL'^2}{K_{aq}} + h_{river}^2} \quad (5)$$

Where h_{aq} represents the aquifer head (m), which is fixed prior to river routing, W represents the recharge rate (mm), L' means the aquifer width of 25 m (CPRM (2014, 2015)), and K_{aq} represents the hydraulic conductivity of the aquifer (mm/d). Negative values of h_{aq} (m) correspond to an aquifer stage below the river bottom. Previous research has demonstrated that groundwater levels in the alluvial aquifer of the semi-arid region of Ceará, Brazil, range from -1 to -20 meters below the surface (Alves *et al.* (2024)). Therefore, the h_{aq} value is the reverse of equation 5 for previous non-intense rainfall events (p < 10 mm/day), as the values would fall within that interval. The recharge rate (W) was estimated as 20% of the rainfall for alluvial areas within dryland regions (Andualem *et al.* (2021)).

The difference between h_{aq} and h_{river} results in the head difference (Δh). By applying Darcy's law, the flow between the aquifer and the river can be calculated (equation 6), where the negative sign indicates that water moves towards the decreasing hydraulic head (Sophocleous (2002)).

$$q_{head} = -K_{aq} \cdot A_{lk} \cdot \frac{\Delta h}{L'} \quad (6)$$

Where A_{lk} represents the cross-sectional area available for flow (m^2), and positive values in equation 6 indicate a contribution from the aquifer to the river as baseflow. In contrast, negative values indicate the opposite direction, contributing to the aquifer recharge. Equation 7, adapted from

Watson et al. (2021) by incorporating a negative sign, calculates the seepage volume in the river reach, contributing downstream as a hyporheic flow.

$$q_{sp} = -min\ (I_t; K_{rb} \cdot sink_a \cdot R_h^2 \cdot \Delta x) \quad (7)$$

In equation 7, K_{rb} represents the hydraulic conductivity of the riverbed (m/d), R_h is the hydraulic radius of the river cross-section (m), and $sink_a$ is a scaling parameter, which is assumed to be equal to the hydraulic radius. Finally, the sum of q_{head} (m^3/s) and q_{sp} (m^3/s) yields the total groundwater flow (equation 8) for the river-aquifer interaction estimation (Ω). After computing Ω, flood wave routing was applied using the previously mentioned nonlinear Muskingum-Cunge equation (equation 1) to determine the outflow at each river reach.

$$\Omega = q_{head} + q_{sp} \quad (8)$$

Natural transmission losses and performance criteria

A form of direct global assessment of the relevance of transmission losses in relation to the inflow and outflow in the river reach at each Δt time step (R) is shown in Equation 9. Because sub-catchment runoff can influence the calculation of the transmission losses, R was not computed for μ values greater than 4% of the inflow in the river reach (I_t).

$$R = (Q_{t+\Delta t} - I_t) / I_t \quad (9)$$

Where $R \geq 0$ may indicate null, compensated or exceeded transmission losses by sub-catchment runoff between stream gauges, but also the recharging of the reach through the subsurface flow or baseflow (Musy e Higy 2011). Negative R values show the loss of river flow to the aquifer (Izady *et al.* (2014)).

Finally, the calibration period was divided into two intervals: period 1, from 04 January 2022 to 21 June 2022 (169 daily streamflow measurements); period 2, from 04 January 2023 to 09 May 2023 (126 daily streamflow measurements). Then, the model calibrated with period 1 was cross-validated using data from period 2 and vice versa. During the calibration process, our objective was to match the simulated streamflow with daily measurements obtained from the river gauges in the Middle Jaguaribe River. Three commonly used statistical measures in hydrological modelling were employed as performance criteria: the Kling-Gupta Efficiency (KGE), the Nash-Sutcliffe Efficiency (NSE), and the percent bias (PBIAS).

RESULTS

These results were derived from the daily streamflow and river stage measurements of each stream gauge during Periods 1 and 2 (Figure 1). Subsequently, these measurements were used to propose a conceptual model, validate the numerical model, and ensure its accuracy. In particular, there was a trend toward river losses between N1-N2 and N3-N4 and river gains between N2-N3 in both periods.

Figure 1 - Observed streamflow (a) and river stage head (b) series during Period 1 (2022) and Period 2 (2023)

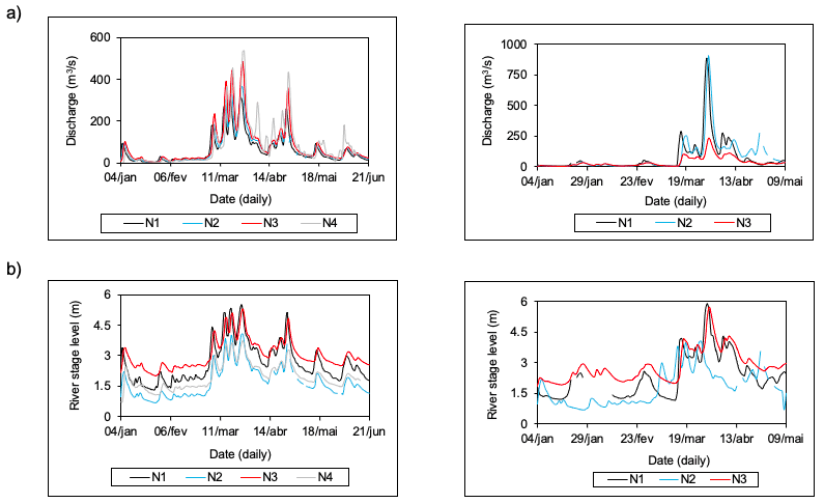

Conceptual model

Transmission losses occurred mostly at the beginning of the rainy season (-1.0 < R < 0.0). Transmission gains (R > 0) were influenced by intense rainfall events (>20 mm/d), where outflow in N4 gauge more than doubled in relation to inflow (close to events of intense rainfall or influence from river reach 02). A trend was observed where higher river stage levels and flow rates in the reaches resulted in increased rates of transmission gains downstream (R > 0.0). This finding highlights the more significant influence of river flow on transmission losses compared to seasonality.

The conceptual model for river-aquifer dynamics at the study site is described as follows: The longitudinal valley has approximately the same slope as the Jaguaribe river, and the lateral valley has a small slope. These characteristics classify the river as a mixed flow system, alternating the preponderance between the baseflow and the hyporheic flow components (Sophocleous (2002)). The water flow direction and rate (volume/time) in the system depends on the difference in water level between the aquifer and the river (hydraulic gradient) and on the hydraulic conductivity between the riverbed and the associated alluvium. The hydraulic gradient becomes positive during the rainfall season (flow direction: aquifer to river), which is concentrated in the first six months of the year. This results in a rapid rise of the groundwater table, contributing to surface flow through both baseflow and hyporheic flow components. Additionally, there is infiltration of surface water into the aquifer. In the absence of rainfall, more frequent in a semiarid region, the connectivity between the river and the aquifer is disrupted as the groundwater level declines below the river cross-section, with vertical groundwater flow downward (vertical infiltration). Since the hydraulic conductivity of the riverbed is 10^4 times greater than alluvium, there is a significant preferential flow in the river-aquifer direction under the influence of a negative hydraulic gradient.

Calibration and validation

Table 1 presents the calibration and validation performance metrics, with threshold values for satisfactory and unsatisfactory performances. Figures 2 (a, b, c) and 3 (a, b) depict the calibration and validation processes for periods 1-2, respectively. The graphs reveal that the outflow was accurately simulated over the 70 km stretch of the Jaguaribe River, even though no groundwater level data were measured during calibration periods 1 and 2.

Table 1 - Evaluation of the model performance metrics for streamflow at the three river reaches during calibration periods 1 and 2 using two-fold cross-validation of the dataset, where KGE is the Kling-Gupta Efficiency, NSE is the Nash-Sutcliffe Efficiency, and PBIAS is the percent bias

Periods	Process	Statistical criteria	Satisfactory performance*	Reach 1	Reach 2	Reach 3
1	Calibration	KGE	0.51< KGE	0.60	0.01	0.78
		NSE	0.50 < NSE < 0.70	0.63	0.42	0.69
		PBIAS (%)	±15 ≤ PBIAS ≤ ±45	36.91	60.67	13.47
2	Validation	KGE	0.51< KGE	0.56	0.32	
		NSE	0.50 < NSE < 0.70	0.54	0.50	
		PBIAS (%)	±15 ≤ PBIAS ≤ ±45	18.58	22.13	
2	Calibration	KGE	0.51< KGE	0.48	0.51	
		NSE	0.50 < NSE < 0.70	0.51	0.56	
		PBIAS (%)	±15 ≤ PBIAS ≤ ±45	17.22	27.45	
1	Validation	KGE	0.51< KGE	0.54	0.67	
		NSE	0.50 < NSE < 0.70	0.58	0.89	
		PBIAS (%)	±15 ≤ PBIAS ≤ ±45	42.59	26.76	

* Threshold values from Moriasi *et al.* (2015) and Lamontagne *et al.* (2020)

Figure 2 - Observed and estimated daily streamflow at reaches 1 (N1-N2), 2 (N2-N3), and 3 (N3-N4) during the calibration period 1 (from 04 January 2022 to 21 June 2022)

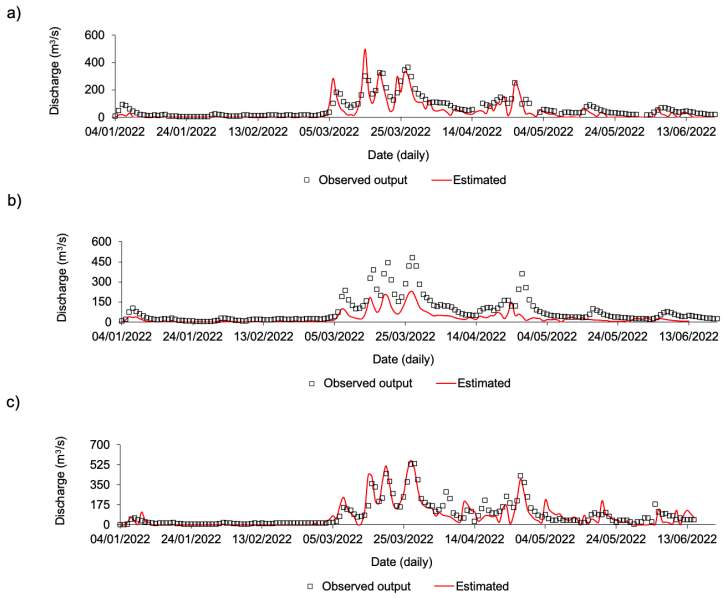

Figure 3 - Observed and estimated daily streamflow at reaches 1 (N1-N2) and 2 (N2-N3) during the validation period 2 (from 04 January 2022 to 21 June 2022)

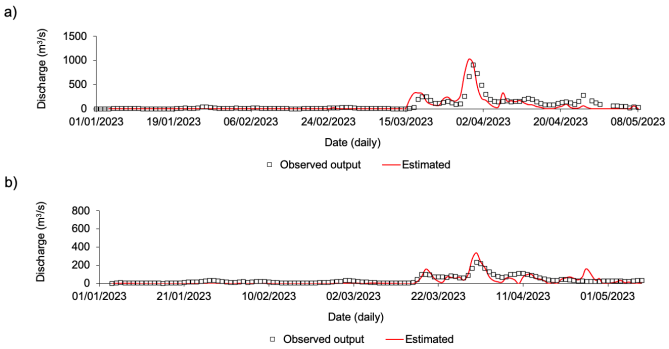

The performance metrics (see Table 1) demonstrated the effectiveness of the model in estimating outflow and capturing peak flow events. The original model (eq. 1) successfully captured the behavior of the observed streamflow curve. The discrepancies between the estimated and observed data in reach 2, such as in the magnitude of peak flows (Figure 2), although small, may be partly explained by the simple equations used to represent groundwater flow, as well as the constant value of the hydraulic conductivity of the river and alluvium. These factors also affect the drops in the recession flow indicated in Figures 2-3, as they are used to calculate the river-aquifer interaction. Numerical models of dryland rivers have revealed similar behavior regarding the decrease in recession flow and the magnitude of peak flows (Kim *et al.* (2022)).

In addition to the outflow, the model also estimates other fluxes, such as river rainfall/evaporation flow, hyporheic flow, and lateral tributary flow, which are sources of groundwater recharge and are essential for a more accurate account of the river water balance. Although these fluxes cause fluctuations in the assumed one-day lag discharge (e.g., after consecutive rainfall and rapid river discharge decrease), introducing uncertainties in the computed outflow, the daily time-step has been demonstrated to be reasonably appropriate to estimate it. Moreover, these computed flows do not require large amounts of data, which is difficult to find in dryland regions (Kim *et al.* (2022)).

River-aquifer interaction

The influence of the sub-catchment runoff and groundwater fluxes can be evaluated by comparing different model structures using the same parameter set. As shown in Data and Methods, the original model employs a river routing equation (eq. 1), which accounts for three key hydrological processes: baseflow, hyporheic flow, and subcatchment runoff (lateral tributary inflow). We tested four model structures using exact spatial discretization and parameter values to assess which combination yielded the most accurate simulation, that is, the best performance metrics. These structures were defined as follows: (1) lateral tributary inflow with both baseflow and hyporheic flow (i.e., the proposed model described in Equation 1) (LTI+BF+HF), (2) lateral tributary inflow with hyporheic flow but without baseflow (LTI+HF), (3) lateral tributary inflow with baseflow but without hyporheic flow (LTI+BF), and (4) baseflow with hyporheic flow but without lateral tributary inflow (BF+HF). Figure 4 shows the observed and simulated streamflow series for each configuration.

Figure 4 - Observed and estimated daily streamflow at reaches 1 (a), 2 (b), and 3 (c) in 2022. The four model structures tested were (1) lateral tributary inflow with both baseflow and hyporheic flow (i.e., the numerical model described in equation 1) (LTI+BF+HF); (2) lateral tributary inflow with hyporheic flow but without baseflow (LTI+HF); (3) lateral tributary inflow with baseflow but without hyporheic flow (LTI+BF); and (4) baseflow with hyporheic flow but without lateral tributary inflow (BF+HF)

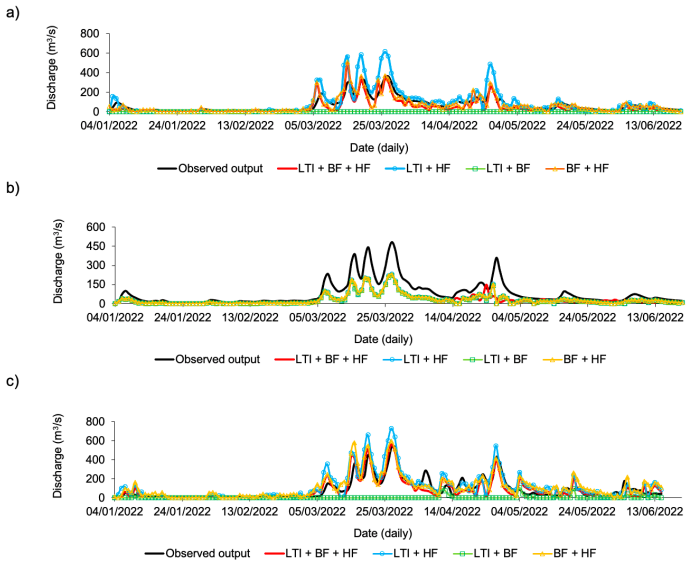

The LTI+HF-based model overestimated the streamflow peaks in reaches 1 and 3, although the difference between the observed and estimated values was not significant. By contrast, the LTI+BF-based model failed to provide accurate streamflow estimates for these reaches. No significant difference was observed between the BF+HF and the LTI+BF+HF-based models (eq. 1) in reaches 1 and 3, respectively. These results suggest a predominant influence of hyporheic flow in these reaches compared to lateral tributary flow and baseflow. However, all four model structures produced similar results for reach 2 (see Figure 4), indicating that inflow dominates in this reach. Among the fluxes, only the baseflow exhibited high sensitivity coefficients for lower and higher values relative to the original. In contrast, hyporheic flow and lateral tributary inflow displayed negligible sensitivity, even for values up to ten times the original. Considering the three reaches, the results suggest that hyporheic flow may be crucial for informing water resource management in dryland rivers.

CONCLUSION

This study developed a simple original model for river-aquifer interactions in dryland rivers. It was designed to address data scarcity and does not require extensive data, such as aquifer head measurements. Because the model also computes other fluxes that influence river-aquifer interactions, such as hyporheic flow, despite its simplicity, it can also contribute to a more accurate water balance between river reaches. The principal findings of this study are summarized as follows.

- A simplified model framework can represent river-aquifer interactions and outflow in dryland rivers at a watershed scale, even without groundwater flow measurements.
- Hyporheic flow, an often-overlooked component of stream aquifer fluxes, may be crucial for water resource management in dryland rivers.
- River loss occurred at the beginning of the rainy season (<10 mm/day), highlighting a greater dependence on river inflow volume and stage rather than intraseasonal rainfall.

REFERENCES

ALVES, R.S.; LINHARES, S.S.; MÖBUS, G. *et al*. (2024). *"Effects of the latest drought on the alluvial aquifer of a semiarid region in northeastern Brazil"*. Proc IAHS 385, pp. 225–229.

ANA. (2018). *Curve Number da Base Hidrográfica Ottocodificada*. Catálogo Metadados ANA. https://metadados.snirh.gov.br/geonetwork/srv/api/records/d1c36d85-a9d5-4f6a-85f7-71c2dc801a67. Accessed 4 May 2024

ANDUALEM, T.G.; DEMEKE, G.G.; AHMED, I. *et al*. (2021). *"Groundwater recharge estimation using empirical methods from rainfall and streamflow records"*. J Hydrol Reg Stud 37, pp. 100917.

CHEN, C.; HE, W.; ZHOU, H. *et al*. (2020). *"A comparative study among machine learning and numerical models for simulating groundwater dynamics in the Heihe River Basin, northwestern China"*. Sci Rep 10, pp. 3904.

CHESNAUX, R.; MOLSON, J.W.; CHAPUIS, R.P. (2005). *"An Analytical Solution for Ground Water Transit Time through Unconfined Aquifers"*. Groundwater 43, pp. 511-517.

COSTA, A.C.; DUPONT, F.; BIER, G. *et al*. (2023). *"Assessment of aquifer recharge and groundwater availability in a semiarid region of Brazil in the context of an interbasin water transfer scheme"*. Hydrogeol J 31, pp. 751–769.

CPRM - BRAZILIAN GEOLOGICAL SERVICE. (2014). *Mapa geológico: jaguaretama Folha SB.24-X-C-IV*. RIGeo. https://rigeo.sgb.gov.br/bitstream/doc/17779/5/carta_geologica_jaguaretama.pdf. Accessed 5 May 2025

CPRM - BRAZILIAN GEOLOGICAL SERVICE. (2015). *Mapa hidrogeológico: jaguaribe - Folha SB.24*. RIGeo. https://rigeo.sgb.gov.br/bitstream/doc/16585/3/folha_sb24.pdf. Accessed 5 May 2025

FREAD, D.L. (1993) *"Flow Routing", in Handbook of Hydrology*. Ed. por Maidment, D.R. McGraw-Hill, New York-NY, pp 316-345.

HUSSAIN, F.; WU, R.-S.; SHIH, D.-S. (2022). *"Water table response to rainfall and groundwater simulation using physics-based numerical model: WASH123D"*. J Hydrol Reg Stud 39, pp. 100988.

KIM, S.S.H.; HUGHES, J.D.; MARSHALL, L.A. *et al.* (2022). *"Modelling daily transmission losses in basin-scale river system models under changing hydrological regimes"*. Hydrol Process 36, pp. e14625.

LAMONTAGNE, J.R.; BARBER, C.A.; VOGEL, R.M. (2020). *"Improved Estimators of Model Performance Efficiency for Skewed Hydrologic Data"*. Water Res Research 56, pp. e2020WR027101.

LU, C.; JI, K.; WANG, W. *et al*. (2021). *"Estimation of the Interaction Between Groundwater and Surface Water Based on Flow Routing Using an Improved Nonlinear Muskingum-Cunge Method"*. Water Resour Manag 35, pp. 2649–2666.

MORIASI, D.N.; GITAU, M.W.; DAGGUPATI, P. (2015). *"Hydrologic and Water Quality Models: Performance Measures and Evaluation Criteria"*. Trans ASABE 58, pp. 1763–1785.

SOPHOCLEOUS, M. (2002). *"Interactions between groundwater and surface water: the state of the science"*. Hydrogeol J 10, pp. 52–67.

WIEGAND, M.C. (2009). *Proposta metodológica para estimativa da produção de sedimentos em grandes bacias hidrográficas: estudo de caso Alto Jaguaribe, CE*. Dissertation, Universidade Federal do Ceará